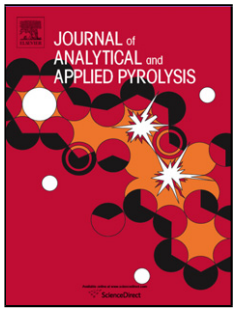

Title: Predicting structural change of lignin macromolecules before and after heat treatment using the pyrolysis-GC/MS technique

Author: Jae-Young Kim Hyewon Hwang Jeesu Park Shinyoung Oh Joon Weon Choi

PII: S0165-2370(14)00241-1
DOI: http://dx.doi.org/doi:10.1016/j.jaap.2014.09.020
Reference: JAAP 3295

To appear in: *J. Anal. Appl. Pyrolysis*

Received date: 23-4-2014
Revised date: 19-9-2014
Accepted date: 24-9-2014

Please cite this article as: J.-Y. Kim, H. Hwang, J. Park, S. Oh, J.W. Choi, Predicting structural change of lignin macromolecules before and after heat treatment using the pyrolysis-GC/MS technique, *Journal of Analytical and Applied Pyrolysis* (2014), http://dx.doi.org/10.1016/j.jaap.2014.09.020

Journal of Analytical and Applied Pyrolysis

Predicting structural change of lignin macromolecules before and after heat treatment using the pyrolysis-GC/MS technique

Jae-Young Kim[a], Hyewon Hwang[a], Jeesu Park[a], Shinyoung Oh[a], Joon Weon Choi[a*]

[a]Department of Forest Sciences and Research Institute for Agriculture and Life Science, Seoul National University, 599 Gwanak-ro, Gwanak-gu, Seoul, 151-921, Korea

*Corresponding author. Tel: +82-2-880-4788; Fax: +82-2-873-2318
E-mail address: cjw@snu.ac.kr

ABSTRACT

Milled wood lignin extracted from poplar wood was subjected to a heat treatment in the temperature range of 150 to 300 °C at 50 °C intervals. The results of several chemical characterizations (proton nuclear magnetic resonance (^{1}H-NMR), derivatization followed by reductive cleavage (DFRC), elemental composition) and thermogravimetric analysis revealed that cleavage of the β-O-4 linkage accompanied by condensation and a charring reaction occurred during the heat treatment, leading to the formation of a thermally-stabilized lignin at 300 °C (300-L) with enrichment of the condensed carbon-carbon bond. Pyrolysis-GC/MS data showed that 41 kinds of pyrolysis products, mainly composed of monomeric phenols, were released from the heat-treated lignin, and the yield of such products was significantly dependent on the lignin sample and the pyrolysis temperature. The maximum yield of total pyrolysis products from 300-L was obtained at a pyrolysis temperature of 600 °C, whereas the maximum yield from the other samples was observed at 500 °C due to the high thermal stability and degree of condensation of 300-L. Moreover, the pyrolysis-GC/MS results suggested that the side chain in the phenol skeleton (C3C6) was considerably degraded at 300 °C, resulting in the accumulation of a C6/C1C6/C2C6-type lignin structure in the 300-L sample. With an increase in the pyrolysis temperature, the syringyl/guaiacyl (S/G) ratio of all lignin samples, as determined from the pyrolysis products, constantly decreased due to an increase in G-type compounds released in the high temperature region.

Keywords: Lignin, Torrefaction, Heat-treatment, TGA, DFRC, Pyrolysis-GC/MS

1. Introduction

Lignin is the second most abundant natural polymer after cellulose, and it accounts for 10-30 wt% of lignocellulosic biomass. Structurally, lignin is a three-dimensional amorphous macromolecule consisting of three types of monolignols (*p*-coumaryl alcohol, coniferyl alcohol, and sinapyl alcohol) with various inter-unit linkages, including ether linkages (e.g., α-O-4, 5-O-4, and β-O-4) and condensed linkages (e.g., 5-5, β-β, β-5, and β-1 linkages) [1]. Recently, many researchers have shown an increased interest in lignin utilization because approximately 50 million tons of lignin is produced globally each year as a by-product, especially from chemical pulping processes in the pulp and paper industry [2]. Due to the inherent structural properties of lignin (a phenolic polymer), the application of lignin to value-added materials (e.g., stabilizers, carbon fibers, dispersing agents, thermoplastics, and fusible materials) or fuel/aromatic chemicals has been widely studied [3-6].

The structural characteristics of lignin, especially the contents of its functional group, the molecular weight, elemental composition, and thermal decomposition properties, are an important factor in determining the physicochemical properties of the target products. Kubo and Kadla [7] investigated the effect of the biphenolic structure of lignin on the blend miscibility and polymer–polymer interactions. The researchers reported that the flexible alkoxyl moiety in the C_α and C_γ positions of the lignin side chain enhanced the thermal mobility of the lignin [8]. Saraf and Glasser found that the phenolic hydroxyl content and the molecular weight of lignin had a profound effect on the tensile strength of lignin-based polyurethane films [9]. In addition, thermally-modified lignin having a low hydroxyl content and a condensed structure was advantageous to the production of lignin-based carbon fiber [4]. Therefore, an in-depth study of the structural features and thermal decomposition

properties of lignin must be conducted before its widespread utilization.

Pyrolysis–GC/MS is a powerful analytical tool that can be applied to investigate the lignin structure based on the pyrolysis products, specifically with regards to the proportion of H-, G-, and S-type monomeric phenols [10]. During pyrolysis, lignin is thermally degraded to low molecular weight phenols by exposure to heating in an inert atmosphere, and these pyrolysis products provide information on the structure of the lignin [11]. The method also has several analytical advantages, including simple preparation with a small sample quantity (μg scale) and rapid analysis times [12]. In recent years, interest in the lignin or biomass structure using pyrolysis–GC/MS analysis has increased [13-16].

The use of heat treatment is one technique to modify the chemical and structural characteristics of **biomass. Torrefaction is a one of thermal pretreatment process performed in the temperatures of 200 – 300 °C under an inert atmosphere to improve energy density of biomass [17]. Prins et al. [18] reported that the kinetics of torrefaction reactions of hemicellulose and cellulose in the temperature range of 230 – 300 °C. This study highlighted that hemicellulose was much easily decomposed than cellulose. In the perspective of lignin, acting as glue in torrefied biomass,** many previous studies revealed that the cleavage of β-O-4 linkages (depolymerization) coupled with condensation, a change in the functional group content, the formation of cross-linking, and loss of the oxygenated structure occurred upon the application of a heat treatment [19-22]. However, these studies used the entire biomass as the raw material and thus, there is a lack of research dealing with only the lignin fraction after heat treatment. Furthermore, far too little attention has been paid to investigating the heat-treated lignin structure via the pyrolysis-GC/MS technique. In this study, only the lignin fraction extracted from poplar wood (milled wood lignin: MWL) was subjected to a heat treatment. These samples were then analyzed by several chemical/thermal

characterization methods and a pyrolysis-GC/MS instrument so as to predict the structural change in the lignin after heat treatment.

2. Materials and Methods

2.1 Preparation of milled wood lignin and heat treatment of the lignin

MWL, one of the representative native lignins, was extracted from poplar wood xylem (*P. albaglandulosa*) based on the Bjorkman method [23]. The yield of MWL was ca. 5.5 % based on the dry weight of the poplar wood xylem. Details of the heat treatment process were described in previous work [24]. Briefly, 100 ± 5 mg of MWL was introduced into a cylindrical glass tube and a thermal treatment was carried out with a CDS Pyroprobe 1500 interface (CDS Analytical, Oxford, PA, USA) under a sufficient flow of helium. The heat treatment temperature was varied from 150 to 300 °C at 50 °C intervals with the treatment time fixed at 10 min. The lignin heat-treated at different temperatures are abbreviated as control (MWL), 150-L (150 °C), 200-L (200 °C), 250-L (250 °C), and 300-L (300 °C).

2.2 Derivatization followed by reductive cleavage (DFRC)

To investigate the frequency of arylglycerol-b-aryl ether linkages (β-O-4), heat-treated lignin samples were examined by the DFRC method [25]. As essential DFRC products, acetylated coniferyl (G–CH=CHCH$_2$OAc) and sinapyl alcohol (S–CH=CHCH$_2$Oac) were produced and their amounts were quantitatively determined by the GC analysis method, as reported in previous research [26].

2.3 ^{1}H-NMR

Proton nuclear magnetic resonance (^{1}H-NMR) spectra were obtained with a Bruker

AVANCE 600 spectrometer (Bruker, Germany). For these experiments, 150 mg of heat-treated lignin dissolved in DMSO-d_6 was analyzed at an operating temperature of 60 °C with 128 scans.

2.4 Thermal decomposition analysis

The thermal decomposition properties of the heat-treated lignin were determined via thermogravimetric analysis (TGA). **In this analysis, sample under 500 µm was selectively used.** The TGA was carried out at three different heating rates of 10, 100, and 200 °C/min up to a temperature of 800 °C. During the analysis, a continuous flow of N_2 gas (25 mL/min) was maintained to ensure an inert atmosphere.

2.5 Pyrolysis-GC/MS analysis

To begin, 1.00 ± 0.05 mg of heat-treated lignin was introduced into a **quartz** tube with a 1 µL internal standard (IS: 1.3 mg of fluoranthene/mL **in methanol**), followed by drying in a vacuum desiccator for 24 h to remove any water or solvent in the prepared samples. The samples were pyrolyzed at various temperatures (400 to 600 °C at 50 °C intervals and 700 °C) with a 10 °C/ms heating rate in an inert atmosphere (>99.9% He) using a CDS Pyroprobe 2000 (CDS Analytical Inc., Oxford, PA, USA); the pyrolysis time was fixed at 20 s. The released volatile products were analyzed online using a gas chromatograph (Agilent Technologies 7890A) equipped with a mass **spectrometer** detector (Agilent Technologies 5975A). A DB-5 capillary column (60 m × 0.25 mm ID × 0.25 µm film thickness) was employed for volatile product separation with a split ratio of 1:200. The pyrolyzer interface, a gas chromatograph injector, and the detector temperatures were set to 300, 320, and 300 °C, respectively. The oven temperature program started at 50 °C for 1 min, followed by a ramp

up to 130 °C at a heating rate of 3 °C/min, and a further increase to 180 °C at a rate of 1.5 °C/min. Next, the temperature was raised to 280 °C at a rate of 6 °C/min and maintained for 5 min. Finally, the temperature was increased to 320 °C for 10 min. The mass spectra of each compound were identified according to NIST MS Search 2.0 (NIST/EPA/NIH Mass Spectral Library; NIST 02) with a proper reference [27]. For quantification of the identified compounds, 18 types of authentic compounds (phenol, guaiacol, 4-methylguaiacol, 3-methoxy-1,2-benzenediol, 4-ethylguaiacol, 4-vinylguaiacol, syringol, 4-propylguaiacol, vanillin, isoeugenol, 4-methylsyringol, acetoguaiacon, 4-ethylsyringol, 4-vinylsyringol, syringaldehyde, methoxyeugenol, coniferaldehyde, and sinapadehyde) were purchased from Sigma Aldrich and injected into the GC-FID to determine the response factor (RF) between each authentic compound and the IS [28]. **Detailed method for quantification of each compound is described in supplementary information.**

3. Results and discussion

3.1 Structural characteristics of heat-treated lignin

In our earlier study, we reported that a weight loss of up to 19% (300 °C) occurred during heat treatment due to a loss of terminal phenolic groups in the lignin polymer and cleavage of the side chain (C3: C_α-C_β-C_γ) from the phenol skeleton (C6) [24]. In addition, a visual color change was noted in the lignin before and after heat treatment (as shown in Fig. S1). Therefore, spectroscopic (^{1}H-NMR), elemental, and DFRC analyses were carried out to investigate structural changes in the lignin after the heat treatment.

Fig. S2 shows the ^{1}H-NMR results obtained for the heat-treated lignin. Firstly, it could be confirmed that 250-L and 300-L had broader and less sharp peaks when compared to the other samples because of their low solubility **in** DMSO-d_6. This implies that the structural

rearrangement of the lignin occurred internally during the heat treatment. Nevertheless, the peaks near 6.7 ppm, derived from aromatic hydrogen, revealed that all heat-treated lignins maintained an aromatic structure. Notably, the peaks originating from H_β and H_γ of the β-O-4 structure gradually decreased and even disappeared for 300-L due to excessive condensation reactions or charring of the lignin [29].

It is well known that the frequency of the β-O-4 linkage, which accounts for 40–65% of lignin, significantly influences the chemical and physical properties of the lignin [30, 31]. Thus, a DFRC analysis was performed to determine the frequency of the β-O-4 linkage in heat-treated lignin; the results are presented in Table 1. As shown in the table, the DFRC products of the heat-treated lignin gradually decreased, whereas the syringyl/guaiacyl (S/G) ratio increased, which is consistent with the findings of previous work [24]. The decrease in DFRC products may be attributed to a concurrent condensation reaction and the cleavage of β-O-4 linkages at high temperature **(Fig. S5)** [32, 33]. In addition, the increase in the S/G ratio with increasing heat treatment temperature is indicative of the preferential contribution of G-type lignin fragments to the condensation reaction, as such fragments have electron-rich positions (C-5), whereas the C-5 position of S-type lignin fragments was substituted with a methoxyl group [34].

A van Krevelen diagram showing the H/C and O/C ratios of the heat-treated lignin is displayed in Fig. 1. From this result, structural changes as well as the various reactions that take place during heat treatment can often be predicted. The MWL from poplar wood (i.e., the control) had H/C and O/C ratios of 1.22 and 0.48, respectively. Such values were higher than those of other technical lignins such as organosolv lignin, ionic liquid lignin, and klason lignin extracted from the same biomass **species** [35]. The obtained results imply that MWL had a relatively less condensed structure than the other lignins. With an elevation of the heat

184 treatment temperature, both the H/C and O/C ratio decreased significantly. As a result, 300-L
185 had the lowest H/C and O/C ratios (1.07 and 0.35, respectively), indicating that the sample
186 had a highly condensed and weakly reactive structure. This structural properties of 300-L
187 were beneficial for the production of carbon fibers [4].
188
189 **3.2 Thermal decomposition behavior of heat-treated lignin**
190 The thermal decomposition behavior of the heat-treated lignin was investigated via TGA
191 under different heating rate conditions (10, 100, and 200 °C/min). Table 2 shows the
192 formation rate of residual char (wt%) in the heat-treated lignin as a function of the heating
193 rate. The formation rate of residual char increased with an elevation of the heat treatment
194 temperature up to 800 °C under all heating rate conditions. From the obtained results, it could
195 be expected that the lignin became more complex with a more condensed structure and a
196 large amount of condensed carbon-carbon bonds (high structural similarity to char) as the
197 heat treatment temperature was increased [36, 37].
198 Table 3 shows the maximum decomposition peak (V_m) and the temperature (T_m)
199 corresponding to V_m in the DTG curves; both the TG and DTG curves are displayed in Fig. 2.
200 In this study, two representative maximum decomposition peaks (V_{m1} and V_{m2}) with their
201 corresponding temperatures (T_{m1} and T_{m2}) were observed (Fig. 2). Regardless of the heating
202 rate, V_{m1} showed a decreasing trend with increasing heat treatment temperature and even
203 disappeared for the 300-L sample, whereas V_{m2} exhibited a gradual increase. It was
204 previously reported that V_{m1} and V_{m2} originated from cleavage of the β-O-4 linkage and
205 highly condensed carbon-carbon bonds, respectively [24, 35]. The results of this study seem
206 to be consistent with those of prior research since the trend in V_{m1} reflected the frequency of
207 the β-O-4 linkage in heat-treated lignins, as determined by the DFRC analysis (Table 1). It is

208 also interesting that an increase in the heating rate resulted in moderate increases of both V_m
209 and T_m (Table 3). According to Caballero et al., an increase in V_m with a rise in the heating
210 rate could be attributed to the facilitation of heat transfer between the surroundings and the
211 internal lignin due to the increased thermal energy [38].
212
213 **3.3 Pyrolysis-GC/MS analysis**
214 To predict the structural features of the heat-treated lignins, a pyrolysis-GC/MS analysis
215 was performed. GC-FID chromatograms of the pyrolysis products released during a 600 °C
216 heat treatment over 20 s for control and 300-L are described in Fig. 3 with compound
217 numbering. A total of 41 kinds of pyrolysis products were identified; the results are provided
218 in Table 4. Based on their phenyl group (C6) structure, the pyrolysis products were classified
219 into three categories (H-, G- and S-type). In addition, these products were additionally
220 divided into four categories (C6: having no side chain, SP: having a saturated aliphatic side
221 chain, UP: having an unsaturated aliphatic side chain and OP: having an oxygenated
222 functional group) on the basis of their side chain type (C3) (Table 4 and Fig. 4). As shown in
223 Fig. 3, phenol (1), 4-methylguaiacol (8), syringol (15), 4-methylsyringol (20),
224 methoxyeugenol (33), and sinapaldehyde (41) were identified as the main pyrolysis products,
225 and the yield of these products was considerably affected by both the lignin sample and
226 pyrolysis temperature. These points are discussed in more detail in the following section.
227
228 **3.4 Predicting the structure of heat-treated lignin based on the pyrolysis products**
229 The yield of pyrolysis products as a function of the pyrolysis temperature is presented in
230 Fig. 5 (products classified into H-, G- and S-types). As seen in Fig. 5(a)-(c), a relatively lower
231 amount of pyrolysis products were released from 300-L in the low temperature region (before

a pyrolysis temperature of 550 °C) when compared to the other lignins, regardless of the compound type. This means that 300-L had relatively higher thermal stability and a more condensed structure when compared to the other samples. The obtained findings supported the data from previous studies, where it was reported that depolymerization as well as excessive condensation occurred simultaneously at high temperature, leading to the formation of a highly condensed lignin structure [21, 22]. Another possible explanation of the results was that the 300-L sample already suffered the loss of volatile compounds such as phenol, benzoic acid, vanillin, eugenol, syringaldehyde, and sinapyl alcohol during the heat treatment [24]. Meanwhile, Fig. 5(d) shows that a relatively higher yield of total pyrolysis products were released from 300-L when compared to the other samples after the 550 °C heat treatment. Furthermore, the maximum yield of pyrolysis products for the control, 150-L-, 200-L, and 250-L samples was obtained at a pyrolysis temperature of 500 °C, whereas that from 300-L was observed at 600 °C. Such a discrepancy could be attributed to the high thermal stability and condensation degree of 300-L. At an elevated temperature of 700 °C, the yield of pyrolysis products decreased for all lignins due to an enhancement in the decomposition of volatiles to low molecular weight gaseous products such as H_2, CH_4, CO, and CO_2 at high temperature [39].

To investigate the behavior of the side chain (C3: C_α-C_β-C_γ) in the phenol skeleton (C6) during the heat treatment, the pyrolysis products were classified into C6, SP, UP, and OP based on their side chain-type. The yield of classified pyrolysis products as a function of the pyrolysis temperature is given in Fig. 6. Hatakeyama and Hatakeyama reported that the molecular motion of lignin was characterized by the type of side chain [40]. For example, rigid groups or cross-linking in the side chain impeded molecular motion and raised the glass transition temperature (T_g), whereas bulky side chains promoted molecular mobility. In

addition, Kubo and Kadla found that the thermal mobility of lignin was considerably affected by the side chain type when lignin was used as a blending material [8]. Therefore, it is very important to understand the side chain behavior during heat treatment for efficient utilization of heat-treated lignin as a value-added resource.

As shown in Fig. 6 (a), the yield of C6 compounds was significantly higher in 300-L when compared to the other samples in the high temperature region (after a pyrolysis temperature of 550 °C). In our previous study, we found evidence for cleavage of the side chain (C_α-C_β-C_γ) from the phenol skeleton (C6) using ^{13}C-NMR analysis, **which could be confirmed by the weakening of signals at 86 – 60 ppm in Fig. S3 [24]**. Thus, it could be assumed that cleavage of the side chain was accelerated at 300 °C, leading to enrichment of the C6-type lignin structure for 300-L. Furthermore, 300-L also yielded a large amount of SP compounds, especially C1C6 and C2C6 compounds, in the high temperature region, whereas the yield of the C3C6 compound was lower than with the other lignins (Fig. S4). This result also supported our prior assumption. Meanwhile, OP compounds from 300-L showed relatively lower yield when compared to the other lignins. Such a finding is in agreement with previous work by Li et al. [41], where it was revealed that the content of oxygenated structures in lignin decreased rapidly with the release of H_2O, CO, and CO_2, especially above 290 °C.

3.5 Determination of the S/G ratio of heat-treated lignin

The S/G ratios of heat-treated lignin were determined at all pyrolysis temperatures; the results are presented in Table 5. It has previously been reported that several wet chemistry methods, including thioacidolysis, permanganate oxidation, and nitrobenzene oxidation could be employed to determine the S/G ratio of lignin [42-44]. However, these techniques require

long and laborious sample preparation procedures and large sample quantities [45, 46]. In contrast, pyrolysis-GC/MS is known as a quick and highly sensitive method for investigating the S/G ratio with only a small sample amount (μg scale).

Prior studies have noted the importance of the pyrolysis temperature when investigating the S/G ratio because the relative amounts of H-, G-, and S-type compounds from lignin may vary significantly depending on the temperature at which pyrolysis is conducted [35, 47]. In the current study, the S/G ratio of heat-treated lignin was also influenced by the pyrolysis temperature. Specifically, the S/G ratio of 300-L drastically decreased from 3.6 (400 °C) to 1.9 (700 °C) with an increase in the pyrolysis temperature, while the ratio of the other lignins varied from 2.4 to 1.9 for the control, 2.3 to 1.9 for 150-L, 2.4 to 1.8 for 200-L, and 3.0 to 1.8 for 250-L. The abnormally high S/G ratio of 300-L in the low temperature region could be attributed to a G-type lignin fragment with a thermally stable structure that is predominantly connected with condensed carbon-carbon bonds, whereas the S-type lignin fragment had a relatively less condensed structure. Therefore, S-type compounds such as syringol, syringaldehyde, methoxyeugenol, and sinapadehyde were more easily released in the lower temperature region (400 – 450 °C). When the pyrolysis temperature was increased, the S/G ratios of all lignins was reduced due to an increase in G-type compounds from the promotion of cleavage of condensed carbon-carbon bonds between G-type lignin fragments at high temperature. At a pyrolysis temperature of 700 °C, all lignins had an S/G ratio of 1.8 – 1.9, suggesting that this temperature was not suitable for determining the S/G ratio. The reason for this result is not clear, but it may be due to further decomposition of volatiles to gaseous products at high temperature.

4. Conclusion

Heat-treated lignins produced at different temperatures (150, 200, 250, and 300 °C) were subjected to chemical/thermal and pyrolysis-GC/MS analyses in order to investigate their structural characteristics. Among the heat-treated lignins, 300-L showed the highest thermal stability as well as the greatest degree of condensation with the smallest H/C and O/C ratios. Pyrolysis-GC/MS showed that phenol, 4-methylguaiacol, syringol, 4-methylsyringol, methoxyeugenol, and sinapaldehyde were the major pyrolysis products and their yields were clearly influenced by the lignin sample and the pyrolysis temperature. Due to cleavage of the side chain at 300 °C, 300-L yielded a higher amount of C6/C1C6/C2C6 compounds than the other lignins in the high pyrolysis temperature region (after 550 °C). The S/G ratio of lignins was also determined based on pyrolysis-GC/MS experiments, indicating that the value of this parameter varied not only due to the lignin sample, but also the pyrolysis temperature.

Acknowledgement

This research was supported by the Basic Science Research Program through the National Research Foundation (NRF) of Korea, funded by the Ministry of Education, Science and Technology (MEST), Republic of Korea (NRF-2012R1A1A2038676).

Reference

[1] G. Brunow and K. Lundquist, *Functional groups and bonding patterns in lignin (including the lignin-carbohydrate complexes)*, CRC Press, 2010.

[2] S. Cheng, C. Wilks, Z. Yuan, M. Leitch and C.C. Xu, Hydrothermal degradation of alkali lignin to bio-phenolic compounds in sub/supercritical ethanol and water–ethanol co-solvent, Polymer Degradation and Stability 97 (2012) 839-848.

[3] J.H. Lora and W.G. Glasser, Recent industrial applications of lignin: a sustainable alternative to nonrenewable materials, Journal of Polymers and the Environment 10 (2002) 39-48.

[4] J. Kadla, S. Kubo, R. Venditti, R. Gilbert, A. Compere and W. Griffith, . Lignin-based carbon fibers for composite fiber applications, Carbon 40 (2002) 2913-2920.

[5] S. Kubo and J. Kadla, Lignin-based carbon fibers: Effect of synthetic polymer blending on fiber properties, Journal of Polymers and the Environment 13 (2005) 97-105.

[6] J.-Y. Kim, S. Oh, H. Hwang, T.-s. Cho, I.-G. Choi and J.W. Choi, Effects of various reaction parameters on solvolytical depolymerization of lignin in sub-and supercritical ethanol, Chemosphere 93 (2013) 1755-1764.

[7] S. Kubo and J.F. Kadla, Kraft lignin/poly (ethylene oxide) blends: Effect of lignin structure on miscibility and hydrogen bonding, Journal of Applied Polymer Science 98 (2005) 1437-1444.

[8] S. Kubo and J.F. Kadla, Poly (ethylene oxide)/organosolv lignin blends: relationship between thermal properties, chemical structure, and blend behavior, Macromolecules 37 (2004) 6904-6911.

[9] V.P. Saraf and W.G. Glasser, Engineering plastics from lignin. III. Structure property relationships in solution cast polyurethane films, Journal of Applied Polymer Science 29 (2003) 1831-1841.

[10] A.V. Marques and H. Pereira, Lignin monomeric composition of corks from the barks of *Betula pendula*, *Quercus suber* and *Quercus cerris* determined by Py–GC–MS/FID, Journal of Analytical and Applied Pyrolysis 100 (2013) 88-94.

[11] T. Ohra-aho, F. Gomes, J. Colodette and T. Tamminen, S/G ratio and lignin structure among Eucalyptus hybrids determined by Py-GC/MS and nitrobenzene oxidation, Journal of Analytical and Applied Pyrolysis 101 (2013) 166-171.

[12] J. Rodrigues, D. Meier, O. Faix and H. Pereira, Determination of tree to tree variation in syringyl/guaiacyl ratio of *Eucalyptus globulus* wood lignin by analytical pyrolysis, Journal of Analytical and Applied Pyrolysis 48 (1999) 121-128.

[13] X. Gu, X. Ma, L. Li, C. Liu, K. Cheng and Z. Li, Pyrolysis of poplar wood sawdust by TG-FTIR and Py–GC/MS, Journal of Analytical and Applied Pyrolysis 102 (2013) 16-23.

[14] M. Brebu, T. Tamminen and I. Spiridon, Thermal degradation of various lignins by TG-MS/FTIR and Py-GC-MS, Journal of Analytical and Applied Pyrolysis 104 (2013) 531-539.

[15] G. Lv and S. Wu, Analytical pyrolysis studies of corn stalk and its three main components by TG-MS and Py-GC/MS, Journal of Analytical and Applied Pyrolysis 97 (2012) 11-18.

[16] Y. Huang, Z. Wei, Z. Qiu, X. Yin and C. Wu, Study on structure and pyrolysis behavior of lignin derived from corncob acid hydrolysis residue, Journal of Analytical and Applied Pyrolysis 93 (2012) 153-159.

[17] W.-H. Chen and P.-C. Kuo, Torrefaction and co-torrefaction characterization of hemicellulose, cellulose and lignin as well as torrefaction of some basic constituents in biomass, Energy 36 (2011) 803-811.

[18] M.J. Prins, K.J. Ptasinski and F.J. Janssen, Torrefaction of wood: Part 1. Weight loss kinetics, Journal of Analytical and Applied Pyrolysis 77 (2006) 28-34.

[19] B. Tjeerdsma, M. Boonstra, A. Pizzi, P. Tekely and H. Militz, Characterisation of thermally modified wood: molecular reasons for wood performance improvement, European Journal of Wood and Wood Products 56 (1998) 149-153.

[20] M. Hakkou, M. Pétrissans, A. Zoulalian and P. Gérardin, Investigation of wood wettability changes during heat treatment on the basis of chemical analysis, Polymer Degradation and Stability 89 (2005) 1-5.

[21] H. Wikberg and S. Liisa Maunu, Characterisation of thermally modified hard-and softwoods by ^{13}C CPMAS NMR, Carbohydrate Polymers 58 (2004) 461-466.

[22] N. Brosse, R. El Hage, M. Chaouch, M. Pétrissans, S. Dumarçay and P. Gérardin, Investigation of the chemical modifications of beech wood lignin during heat treatment, Polymer Degradation and Stability 95 (2010) 1721-1726.

[23] A. Bjorkman, Studies on finely divided wood. Part I. Extraction of lignin with neutral solvents, Svensk Papperstidning-Nordisk Cellulosa 59 (1956) 477-485.

[24] J.-Y. Kim, H. Hwang, S. Oh, Y.-S. Kim, U.-J. Kim and J.W. Choi, Investigation of structural modification and thermal characteristics of lignin after heat treatment, International Journal of Biological Macromolecules 66 (2014) 57-65.

[25] F. Lu and J. Ralph, DFRC Method for Lignin Analysis. 1. New Method for [beta]-Aryl Ether Cleavage: Lignin Model Studies, Journal of Agricultural and Food

Chemistry 45 (1997) 4655-4660.

[26] J.Y. Kim, E.J. Shin, I.Y. Eom, K. Won, Y.H. Kim, D. Choi, I.G. Choi and J.W. Choi, Structural features of lignin macromolecules extracted with ionic liquid from poplar wood, Bioresource Technology 102 (2011) 9020-9025.

[27] O. Faix, D. Meier and I. Fortmann, Thermal degradation products of wood, European Journal of Wood and Wood Products 48 (1990) 281-285.

[28] I.-Y. Eom, J.-Y. Kim, S.-M. Lee, T.-S. Cho, H. Yeo and J.-W. Choi, Comparison of pyrolytic products produced from inorganic-rich and demineralized rice straw (*Oryza sativa L.*) by fluidized bed pyrolyzer for future biorefinery approach, Bioresource technology 128 (2013) 664-672.

[29] R.C. Sun, J. Tomkinson and G. Lloyd Jones, Fractional characterization of ash-AQ lignin by successive extraction with organic solvents from oil palm EFB fibre, Polymer Degradation and Stability 68 (2000) 111-119.

[30] H. Nimz, Beech lignin—proposal of a constitutional scheme, Angewandte Chemie International Edition in English 13 (2003) 313-321.

[31] T. Kishimoto, Y. Uraki and M. Ubukata, Chemical synthesis of β-O-4 type artificial lignin, Organic & Biomolecular Chemistry 4 (2006) 1343-1347.

[32] J.F. Haw, G.E. Maciel and C.J. Biermann, Carbon-13 nuclear magnetic resonance study of the rapid steam hydrolysis of read oak, Holzforschung 38 (1984) 327-331.

[33] J.F. Haw and T.P. Schultz, Carbon-13 CP/MAS NMR and FT-IR study of low-temperature lignin pyrolysis, Holzforschung 39 (1985) 289-296.

[34] A. Guerra, J.P. Elissetche, M. Norambuena, J. Freer, S. Valenzuela, J. Rodríguez and C. Balocchi, Influence of lignin structural features on Eucalyptus globulus kraft pulping, Industrial & engineering chemistry research 47 (2008) 8542-8549.

[35] J.-Y. Kim, S. Oh, H. Hwang, U.-J. Kim and J.W. Choi, Structural features and thermal degradation properties of various lignin macromolecules obtained from poplar wood (*Populus albaglandulosa*), Polymer Degradation and Stability 98 (2013) 1671-1678.

[36] S. Chu, A.V. Subrahmanyam and G.W. Huber, The pyrolysis chemistry of a β-O-4 type oligomeric lignin model compound, Green Chemistry 15 (2013) 125-136.

[37] B. Krieger-Brockett, Microwave pyrolysis of biomass, Research on Chemical Intermediates 20 (1994) 39-49.

[38] J. Caballero, R. Front, A. Marcilla and J. Conesa, Characterization of sewage sludges by primary and secondary pyrolysis, Journal of Analytical and Applied Pyrolysis 40 (1997) 433-450.

[39] R. Li, Z. Zhong, B. Jin and A. Zheng, Selection of temperature for bio-oil production from pyrolysis of algae from lake blooms, Energy & Fuels 26 (2012) 2996-3002.

[40] H. Hatakeyama and T. Hatakeyama, Lignin structure, properties, and applications, in Biopolymers, Springer 2010 1-63.

[41] Y. Li, D. Cui, Y. Tong and L. Xu, Study on structure and thermal stability properties of lignin during thermostabilization and carbonization, International journal of biological macromolecules 62 (2013) 663-669.

[42] T. Ona, T. Sonoda, K. Itoh and M. Shibata, Relationship of lignin content, lignin monomeric composition and hemicellulose composition in the same trunk sought by their within-tree variations in Eucalyptus camaldulensis and E. globulus, Holzforschung 51 (1997) 396-404.

[43] C.-L. Chen, Nitrobenzene and cupric oxide oxidations. Methods in lignin chemistry, Springer, 1992, p. 301.

[44] G. Gellerstedt, Chemical degradation methods: permanganate oxidation. Methods in Lignin Chemistry, Springer, 1992, p. 322.

[45] C.A. Nunes, C.F. Lima, L.C. Barbosa, J.L. Colodette, A. Gouveia and F.O. Silvério, Determination of *Eucalyptus* spp lignin *S*/*G* ratio: A comparison between methods, Bioresource technology 101 (2010) 4056-4061.

[46] H. Yokoi, Y. Ishida, H. Ohtani, S. Tsuge, T. Sonoda and T. Ona, Characterization of within-tree variation of lignin components in Eucalyptus camaldulensis by pyrolysis–gas chromatography, Analyst 124 (1999) 669-674.

[47] M. Brebu and C. Vasile, Thermal degradation of lignin—A review, Cellulose Chemistry & Technology 44 (2010) 353.

Journal of Analytical and Applied Pyrolysis

Predicting structural change of lignin macromolecules before and after heat treatment using the pyrolysis-GC/MS technique

Jae-Young Kim, Hyewon Hwang, Jeesu Park, Shinyoung Oh, Joon Weon Choi

Highlight

- Milled wood lignin was subjected to a heat-treatment at various temperature ranges.
- Structural change of lignin after heat-treatment was investigated by Pyrolysis-GC/MS.
- Pyrolysis products was significantly dependent on the lignin and pyrolysis temperature.
- S/G ratio of all lignins constantly decreased with increasing pyrolysis temperature.
- Heat-treatment at 300 °C formed new condensed sturucture with enrichement of C-C bond.

Table 1. Quantitative analysis of DFRC products of heat-treated lignin

Lignin	Amount (μmol/g sample)[a]		Sum	S/G ratio
	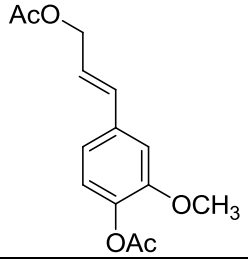	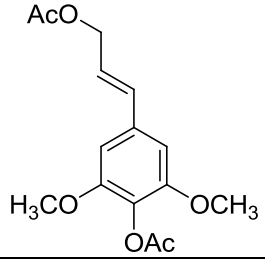		
	Acetylated Coniferyl alcohol.	Acetylated Sinapyl alcohol.		
Control	414.7 (25.7)	561.8 (28.3)	976.6 (52.0)	1.4
150-L	414.4 (22.9)	527.8 (18.6)	942.2 (41.5)	1.3
200-L	229.2 (1.7)	387.5 (12.2)	616.7 (13.9)	1.7
250-L	48.6 (1.0)	113.5 (4.4)	162.1 (5.4)	2.3
300-L	-	-	-	-

[a] Data are means of triplicate analyses with standard deviation in the parenthesis
Ac means acetate group

Table 2. The formation rate of residual char in TG final temperature (800 °C) with applying different heating rate

Lignin	TG - Residual char (wt%)		
	10 °C/min[a]	100 °C/min	200 °C/min
Control	25.6	21.3	20.8
150-L	26.6	24.1	26.6
200-L	24.5	20.7	22.5
250-L	28.4	27.5	31.6
300-L	34.3	33.4	35.0

[a] The results of 10 °C/min were referred from previous study [22]

Table 3. Thermal decomposition characteristics of thermal treated lignin with applying different heating rate

Lignin	DTG											
	10 °C/min[a]				100 °C/min				200 °C/min			
	V_{m1}[b]	T_{m1}[c]	V_{m2}[b]	T_{m2}[c]	V_{m1}	T_{m1}	V_{m2}	T_{m2}	V_{m1}	T_{m1}	V_{m2}	T_{m2}
Control	0.38	290.6	0.36	359.4	0.35	330.2	0.36	402.5	0.34	366.7	0.39	423.1
150-L	0.36	294.0	0.32	358.2	0.37	331.0	0.35	404.2	0.33	366.7	0.38	421.5
200-L	0.38	296.1	0.33	358.9	0.37	332.7	0.39	405.0	0.35	368.3	0.39	423.1
250-L	0.30	308.7	0.38	372.1	0.28	342.7	0.41	408.3	0.33	389.9	0.40	428.1
300-L	-	-	0.42	382.3	-	-	0.47	415.8	-	-	0.50	433.1

[a] The results of 10 °C/min were referred from previous study [22]
[b] V_{m1} and V_{m2} means two maximum degradation peak (wt%/°C) of the former and latter, respectively
[c] T_{m1} and T_{m2} (°C) means the temperature corresponding to V_{m1} and V_{m2} (wt%/°C), respectively

Table 4. Yield of pyrolysis products of thermal treated lignin (600 °C, 20sec)

Peak No.	RT	Pyrolysis products	Type
1	19.9	Phenol	H/C6
2	23.7	3-methyl-phenol (m-cresol)	H/SP
3	24.8	Benzyl alcohol	H/OP
4	25.7	Guaiacol	G/C6
5	28.5	2,4-dimethylphenol	G/SP
6	30.3	6-Methylguaiacol	G/SP
7	30.6	1,2-Benzenediol	G/C6
8	31.0	4-Methylguaiacol	G/SP
9	34.3	3-methyl-1,2-benzenediol	G/SP
10	34.6	3-methoxy-1,2-benzenediol	S/C6
11	35.6	4-Ethylguaiacol	G/SP
12	35.9	4-methyl-1,2-benzenediol	G/SP
13	37.8	4-Vinylguaiacol	G/UP
14	38.1	3-methoxy-5-methyl-phenol	G/SP
15	40.0	Syringol	S/C6
16	40.4	Eugenol	G/UP
17	41.0	4-Propylguaiacol	G/SP
18	43.3	Vanillin	G/OP
19	43.7	Isoeugenol (cis)	G/UP
20	46.1	4-Methylsyringol	S/SP
21	46.6	Isoeugenol (trans)	G/UP
22	46.9	Homovanillin	G/OP
23	48.9	Acetoguaiacon	G/OP
24	50.4	4-hydroxy-benzoic acid	H/OP
25	51.1	4-Ethylsyringol	S/SP
26	51.6	Homovanillic acid	G/OP
27	54.0	4-Vinylsyringol	S/UP
28	55.6	4-(oxo-allyl)-guaiacol	G/OP
29	56.4	4-propenylsyringol (cis)	S/UP
30	56.9	4-propylsyringol	S/SP
31	59.8	4-propenylsyringol (trans)	S/UP
32	60.6	Syringaldehyde	S/OP
33	63.2	Methoxyeugenol	S/UP
34	64.7	Acetosyringone	S/OP
35	65.0	Coniferaldehyde	G/OP
36	65.1	Coniferyl alcohol (trans)	G/OP
37	66.1	Syringyl acetone	S/OP
38	68.3	Propiosyringone	S/OP
39	68.4	4-(oxo-allyl)-syringol	S/OP
40	70.4	Dihydrosinapyl alcohol	S/OP
41	72.9	Sinapaldehyde	S/OP

Table 5. The change in S/G ratio as a function of pyrolysis temperature

	Pyrolysis temperature					
	400 ℃	450 ℃	500 ℃	550 ℃	600 ℃	700 ℃
Control	2.4	1.8	2.2	2.0	1.8	1.9
150-L	2.3	2.2	2.1	2.0	2.0	1.9
200-L	2.4	1.9	2.2	2.1	2.0	1.8
250-L	3.0	2.7	2.4	2.3	2.2	1.8
300-L	3.6	3.0	2.5	2.3	2.2	1.9

Figure 1

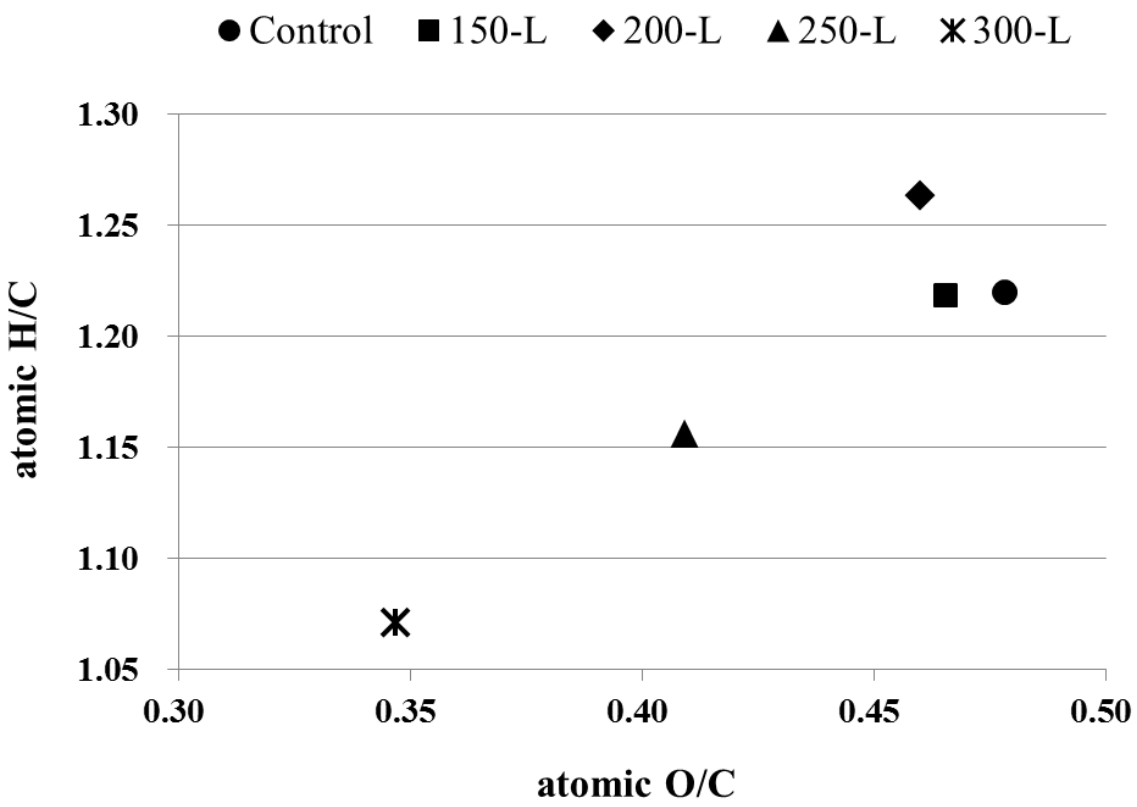

Fig. 1. Van Krevelen diagram of heat-treated lignin

Figure 2

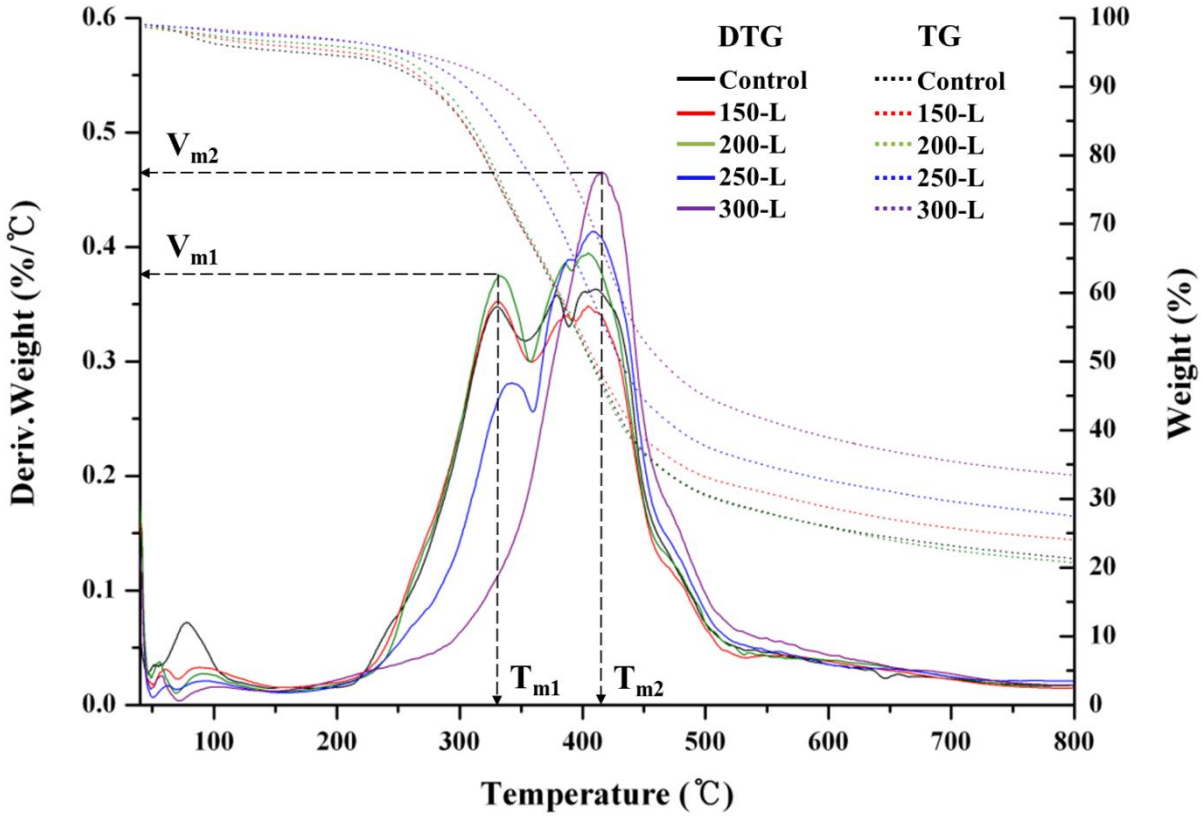

Fig. 2. Thermo Gravimetric (TG) and Derivative TG (DTG) curves of heat-treated lignin (heating rate: 100 °C/min)

Figure 3

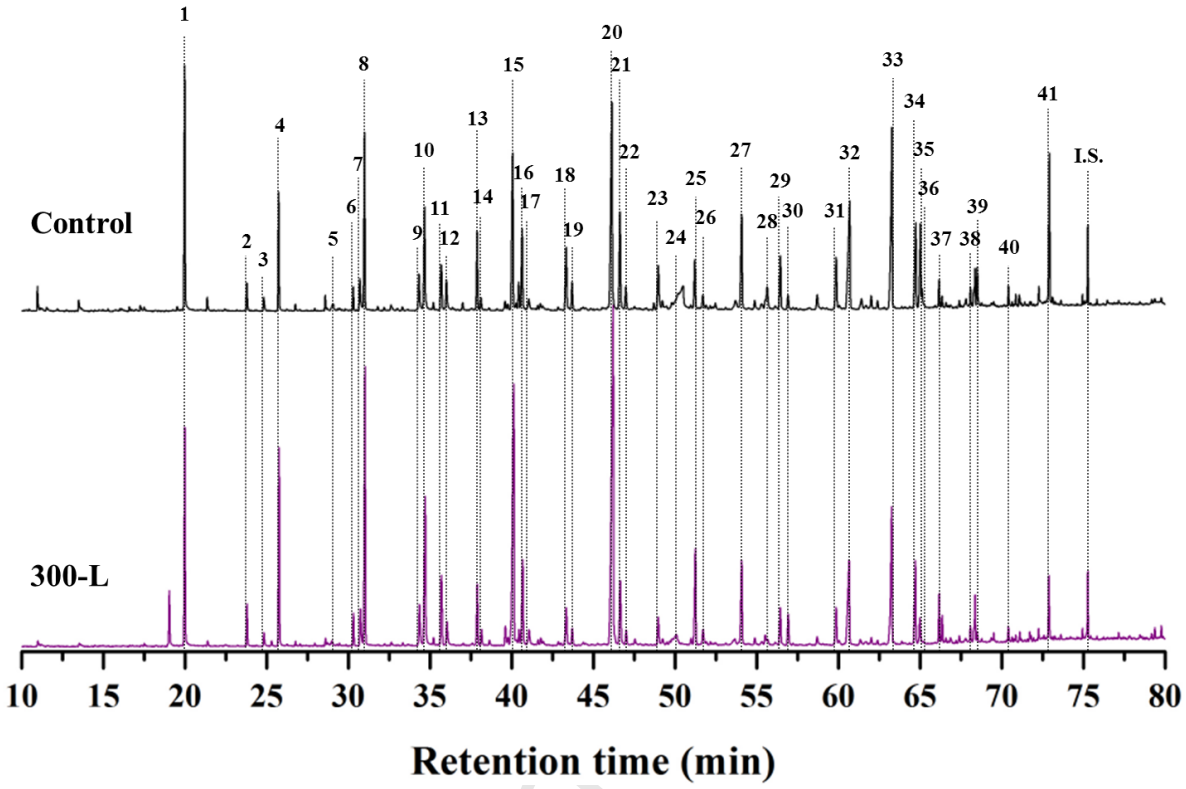

Fig. 3. GC chromatogram of the pyrolysis products from heat-treated lignin (pyrolysis condition: 600 °C, 20 s)

Figure 4

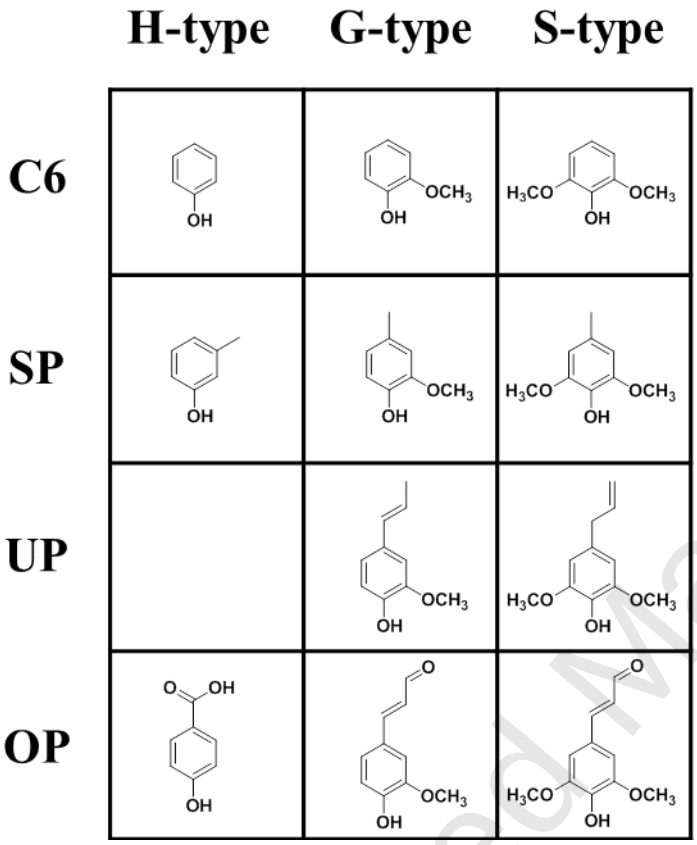

Fig. 4. Molecular structure of classified pyrolysis products

Figure 5

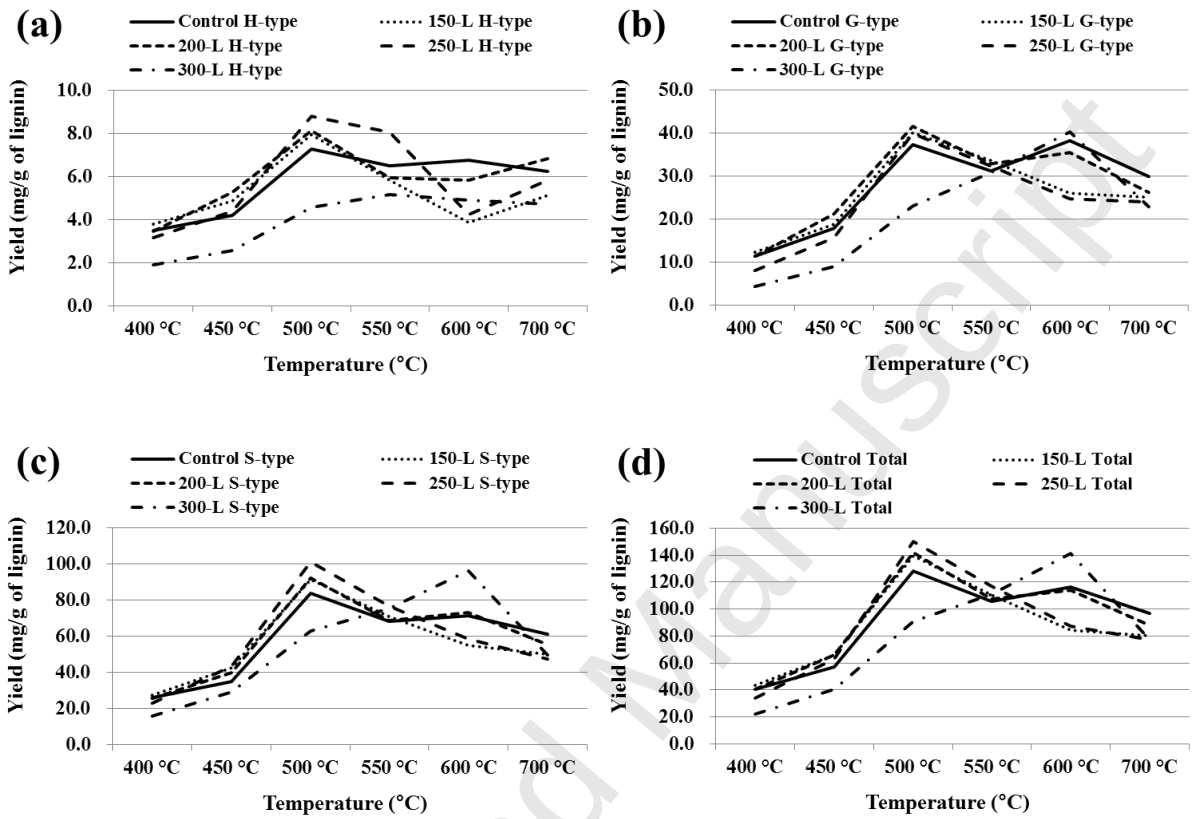

Fig. 5. The change in pyrolysis products yields as a function of pyrolysis temperature (classified into H-, G- and S-type)

Figure 6

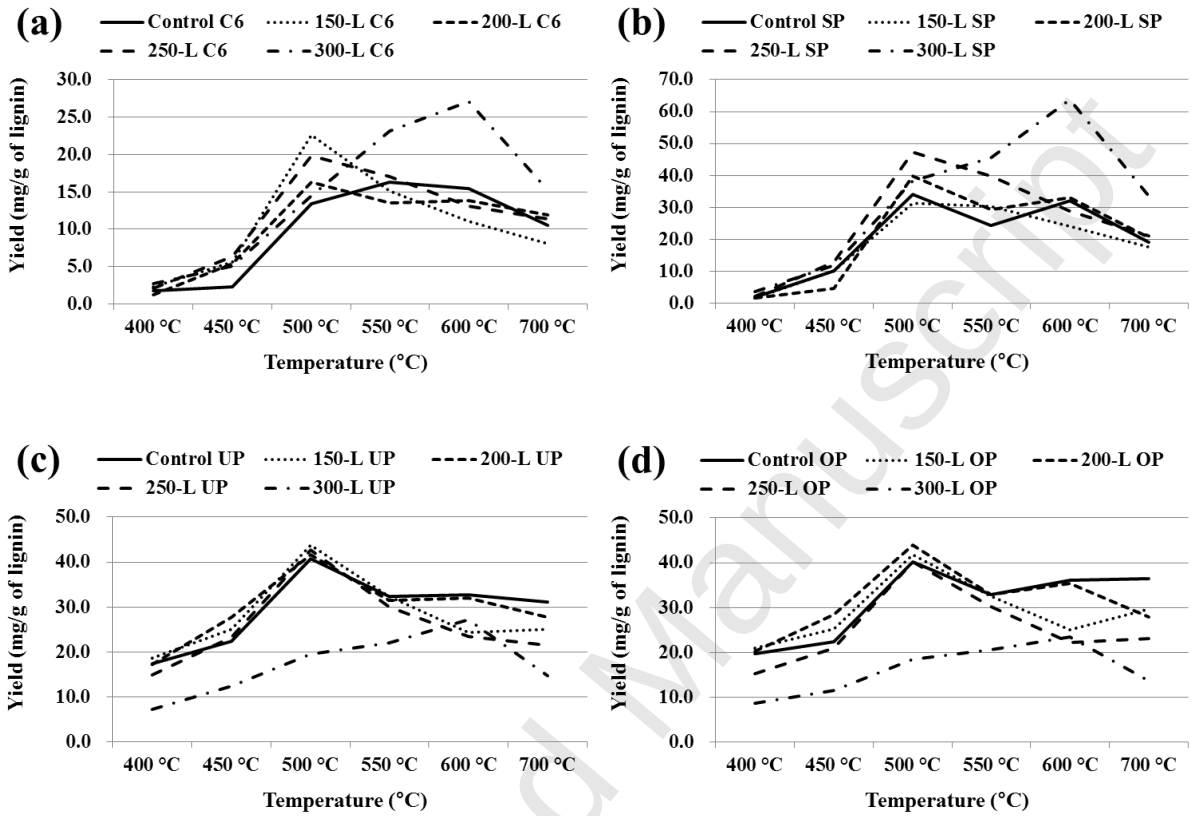

Fig. 6. The change in pyrolysis products yields as a function of pyrolysis temperature (classified into C6, SP, UP and OP)